ISSN 1070-3632, Russian Journal of General Chemistry, 2025, Vol. 95, No. 10, pp. 2900–2910. © Pleiades Publishing, Ltd., 2025.

Methylpiperazine-Based 1,2,4-Triazole Derivatives as Potent DNA Gyrase B Inhibitors with Promising Broad-Spectrum Antimicrobial Activity

Y. U. Cebeci[a,*], Y. K. Karabulut[a], and Ş. Ceylan[b]

[a] *Department of Chemistry, Kırklareli University, Kırklareli, 39100 Turkey*
[b] *Artvin Çoruh University, Faculty of Forestry, Department of Forest Industrial Engineering, Artvin, 08000 Turkey*
**e-mail: y.uyguncebeci@klu.edu.tr*

Received May 5, 2025; revised July 28, 2025; accepted August 7, 2025

Abstract—The emergence of antimicrobial resistance (AMR) poses a critical threat to global health, underscoring the need for new antimicrobial agents. In this study, a novel series of 1,2,4-triazole derivatives was synthesized from methylpiperazine intermediates via esterification, hydrazide formation, thiourea condensation, and Mannich-type reactions. Structural characterization was performed using FT-IR, ^{1}H, ^{13}C NMR, and EI-MS techniques. Antimicrobial activities of the synthesized compounds were evaluated via broth microdilution. One derivative displayed remarkable broad-spectrum activity with MIC values <0.24 μg/mL against *E. coli*, *S. aureus*, *M. smegmatis*, and *C. albicans*. Molecular docking against *E. coli* DNA gyrase B (PDB: 4PRV) revealed strong binding affinities for two derivatives (–9.9 and –9.8 kcal/mol), correlating well with in vitro results. Key interactions included hydrogen bonding, π–π stacking, and halogen bonding. SAR analysis emphasized the role of electron-withdrawing and hydrophobic groups in enhancing activity. These triazole derivatives show promise as potent antimicrobial candidates targeting DNA gyrase B.

Keywords: 1,2,4-triazole, methylpiperazine, antimicrobial activity, DNA gyrase B inhibition, molecular docking, structure–activity relationship (SAR)

DOI: 10.1134/S1070363225602820

INTRODUCTION

The emergence of multidrug-resistant (MDR) bacteria and fungi has become one of the most pressing challenges in global public health, as it threatens the efficacy of existing antimicrobial therapies. The development of novel compounds with unique mechanisms of action is critical to address this issue [1, 2]. Among the chemical scaffolds being explored, the 1,2,4-triazole nucleus has shown significant promise due to its versatile biological activities, including antibacterial, antifungal, antiviral, anticancer, and anti-inflammatory effects [3–6]. Triazole-containing compounds have the potential to overcome resistance by interacting with key microbial targets in unique ways. Triazoles are an integral part of many clinically used drugs, particularly antifungals such as fluconazole and itraconazole [7, 8]. These drugs inhibit the fungal cytochrome P450 enzyme (lanosterol 14α-demethylase), disrupting cell membrane synthesis and leading to cell death. Similarly, triazoles have been explored for their antibacterial activities, with recent studies highlighting their ability to target bacterial enzymes like DNA gyrase and topoisomerase IV [9, 10].

DNA gyrase is a type II topoisomerase that plays a crucial role in bacterial DNA replication, transcription, and repair. Its inhibition results in the accumulation of DNA breaks, leading to bacterial cell death [11–13]. Fluoroquinolones, such as ciprofloxacin, are among the most successful DNA gyrase inhibitors. However, the increasing resistance to fluoroquinolones due to point mutations in the gyrA and gyrB subunits necessitates the discovery of alternative scaffolds targeting this enzyme [14–16].

Recent advancements have focused on 1,2,4-triazole derivatives as potential DNA gyrase inhibitors. For instance, Black et al. synthesized novel triazole-based hybrids that demonstrated nanomolar inhibitory activity against DNA gyrase and potent antibacterial effects against resistant strains [17]. Similarly, Lewis et al.

Scheme 1.

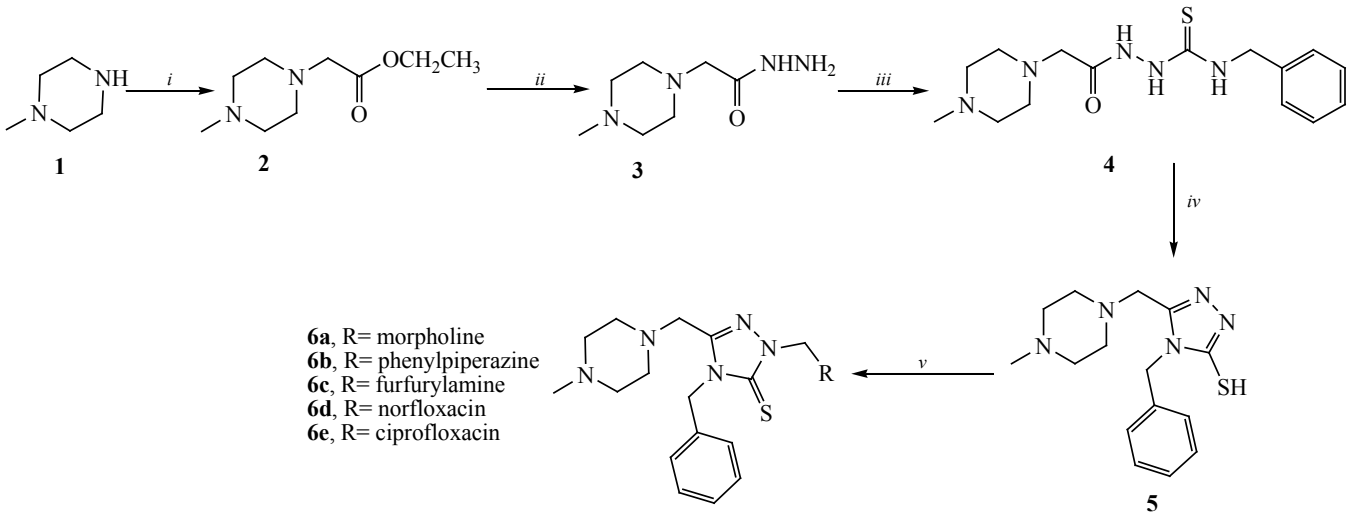

Reagents and conditions: *i*, $BrCH_2COOEt$, EtOH; *ii*, NH_2NH_2, EtOH; *iii*, BnNCS, EtOH; *iv*, NaOH, EtOH, H_2O; *v*, formaldehyde, secondary amine, room temperature, 24 h.

reported triazole derivatives with dual antimicrobial and anticancer activities by targeting multiple biological pathways [18]. These studies underscore the potential of triazole derivatives to serve as multi-targeted therapeutic agents.

The alarming rise in MDR pathogens, such as Escherichia coli, Klebsiella pneumoniae, and Candida albicans, has rendered many existing drugs ineffective [19–21]. Innovative approaches combining synthetic chemistry, molecular modeling, and biological evaluation are required to identify compounds with novel mechanisms of action. Molecular docking has emerged as a powerful tool to predict ligand-target interactions and optimize lead compounds [22–24].

The rationale behind the design of the synthesized 1,2,4-triazole derivatives was based on a structure-guided, bioisosteric replacement approach. The 1,2,4-triazole ring was selected as a core scaffold due to its capacity to form hydrogen bonds and π-interactions with biological targets, enhancing binding affinity and metabolic stability. Methylpiperazine was incorporated to improve aqueous solubility, increase membrane permeability, and introduce basic nitrogen atoms capable of interacting with active site residues. Furthermore, various electron-withdrawing and hydrophobic substituents were introduced at strategic positions to modulate lipophilicity, enhance target binding, and explore structure–activity relationships. This design strategy aimed to optimize both biological activity and pharmacokinetic properties while targeting DNA gyrase B, a well-validated antimicrobial target.

In this study, we synthesized a series of novel 1,2,4-triazole derivatives using a methylpiperazine framework. These compounds were evaluated for their antimicrobial activity against a panel of Gram-positive and Gram-negative bacteria, as well as fungal pathogens. To elucidate their mechanism of action, molecular docking studies targeting *E. coli* DNA gyrase B (PDB ID: 4PRV) were performed. This enzyme was chosen as a target due to its critical role in bacterial survival and its validation as an effective target for antimicrobial agents [25, 26]. The results provide insights into the structural and functional properties of the synthesized compounds, highlighting their potential as antimicrobial drug candidates.

RESULTS AND DISCUSSION

Chemistry. The synthesis of novel 1,2,4-triazole derivatives **2**–**9** was carried out through a series of efficient reactions starting from methylpiperazine (Scheme 1). The first intermediate, ethyl 2-(4-methylpiperazin-1-yl)acetate **2**, was obtained in 89% yield by reacting methylpiperazine with ethyl bromoacetate in the presence of triethylamine. The ester group of compound **2** was subsequently converted into hydrazide **3** via reaction

Scheme 2.

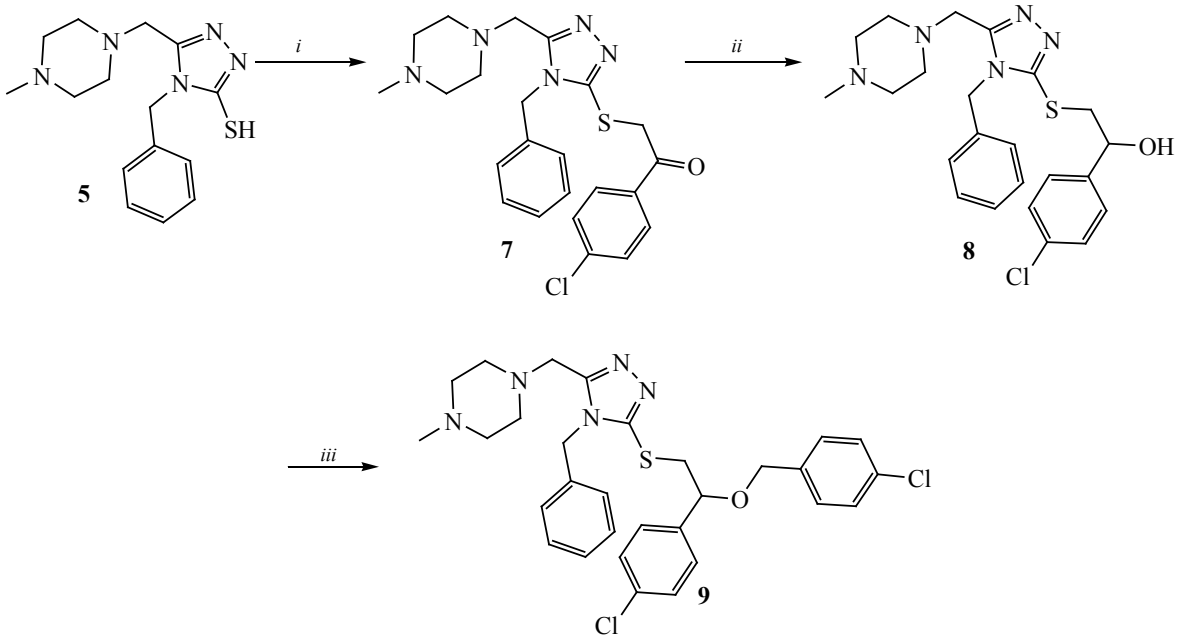

Reagents and conditions: *i*, 2-bromo-1-(4-chlorophenyl)ethanone, NaOEt, reflux; *ii*, $NaBH_4$, EtOH, reflux; *iii*, 4-chlorobenzylchloride, THF, NaH, reflux.

with hydrazine hydrate under reflux conditions, yielding 85% of the desired product. The hydrazide was further reacted with benzyl isothiocyanate in dichloromethane to form *N*-benzyl-2-[(4-methylpiperazin-1-yl)acetyl]-hydrazinecarbothioamide **4** in 81% yield. Cyclization of compound **4** in the presence of NaOH resulted in the formation of 4-benzyl-5-[(4-methylpiperazin-1-yl)-methyl]-4*H*-1,2,4-triazole-3-thiol **5** with a yield of 71%. This compound served as a key intermediate for the synthesis of a series of functionalized triazole derivatives **6a**–**6e** by reacting with formaldehyde and various amines under mild conditions. These derivatives were obtained in high yields (76–91%) and characterized by FT-IR, NMR, and EI-MS, confirming the incorporation of diverse substituents on the triazole ring.

The versatility of the synthetic pathway was further demonstrated by transforming compound **5** into more complex derivatives **7**–**9** through alkylation and reduction reactions. For instance, compound **7** was synthesized by alkylation with 2-bromo-1-(4-chlorophenyl)ethanone, yielding 90% of the product, while compound **8** was obtained via $NaBH_4$-mediated reduction, and compound **9** was prepared through benzylation. The overall synthetic strategy provided efficient access to structurally diverse triazole derivatives, which were obtained in excellent yields and purity. These compounds were characterized by comprehensive spectroscopic analysis, including FT-IR, NMR, and MS, confirming their structures and providing a foundation for subsequent biological and computational studies (Scheme 2).

Antimicrobial activity. The synthesized 1,2,4-triazole derivatives **2**–**9** were evaluated for their antimicrobial activity against a panel of gram-positive and gram-negative bacteria, as well as fungal strains. The results, summarized in Table 1, indicate significant variability in the activity of the compounds depending on their structure and the target microorganism. Compounds **6a**, **6d**, and **6e** demonstrated remarkable broad-spectrum activity with minimal inhibitory concentration (MIC) values of < 0.24 μg/μL against most tested microorganisms, including *Escherichia coli* (*Ec*), *Yersinia pseudotuberculosis* (*Yp*), *Pseudomonas aeruginosa* (*Pa*), *Staphylococcus aureus* (*Sa*), *Enterococcus faecalis* (*Ef*), *Bacillus cereus* (*Bc*), and *Mycobacterium smegmatis* (*Ms*). This highlights their potential as potent antimicrobial agents.

Among the tested compounds, **6d** and **6e** showed superior activity, maintaining MIC values of <0.24 μg/μL against all bacterial strains, while also exhibiting activity against fungal pathogens, such as *Candida albicans*

Table 1. Screening for antimicrobial activity of compounds **2**–**9**

Compound	MIC, μg/μL[a]								
	Ec	*Yp*	*Pa*	*Sa*	*Ef*	*Bc*	*Ms*	*Ca*	*Sc*
2	7.81	7.81	31.25	31.25	62.5	31.25	7.81	–	–
3	–	–	–	–	–	–	–	–	–
4	–	–	–	–	–	–	–	–	–
5	–	–	–	125	–	–	–	250	125
6a	<0.24	<0.24	<0.24	<0.24	<0.24	<0.24	<0.24	–	125
6b	125	125	–	–	–	–	–	–	–
6c	125	125	–	–	–	–	–	–	–
6d	<0.24	<0.24	<0.24	<0.24	<0.24	<0.24	<0.24	62.5	15.65
6e	<0.24	<0.24	<0.24	<0.24	<0.24	<0.24	<0.24	62.5	15.65
7	62.5	125	–	62.5	–	125	15.65	125	62.5
8	31.25	125	–	500	–	125	62.5	125	62.5
9	125	125	125	125	–	125	7.81	125	125
DMSO	125	125	125	–	–	500	125	500	–

[a] *Ec—Escherichia coli* (ATCC35218), *Yp—Yersinia pseudotuberculosis* (ATCC911), *Pa—Pseudomonas aeruginosa* (ATCC43288), *Ef—Enterococcus faecalis* (ATCC29212), *Sa—Staphylococcus aureus* (ATCC25923), *Bc—Bacillus cereus* (709 Roma), *Ms—Mycobacterium smegmatis* (ATCC607), *Ca—Candida albicans* (ATCC60193), and *Sc—Saccharomyces cerevisiae* (RSKK 251).

(*Ca*) (MIC 62.5 μg/μL) and *Saccharomyces cerevisiae* (*Sc*) (MIC 15.65 μg/μL). These findings suggest that the introduction of specific functional groups in the triazole ring enhances both antibacterial and antifungal properties, likely through improved interaction with microbial targets.

In contrast, compound **6a**, despite showing excellent antibacterial activity (MIC <0.24 μg/μL), displayed limited antifungal activity, with a MIC value of 125 μg/μL against *Sc*. Compounds **6b** and **6c** exhibited moderate activity against gram-negative bacteria (*Ec* and *Yp*, MIC: 125 μg/μL), but were inactive against other strains, highlighting the importance of substituent modifications for spectrum broadening. Compound **5**, the precursor in the synthesis, demonstrated weak to moderate activity, particularly against *Ms* (MIC: 125 μg/μL) and *Ca* (MIC: 250 μg/μL), underscoring the role of structural modifications in enhancing antimicrobial potency.

Compounds **7**, **8**, and **9** displayed varied activities, with **7** showing moderate effectiveness against *Ec* and *Bc* (MIC: 62.5 μg/μL) and excellent activity against *Ms* (MIC: 15.65 μg/μL). Compound **8** exhibited weaker activity overall, with MIC values ranging from 31.25 to 500 μg/μL, while **9** showed moderate broad-spectrum activity, particularly against *Ms* (MIC: 7.81 μg/μL). These variations indicate that the nature and position of substituents in the triazole core significantly influence the antimicrobial profile.

The control compounds, dimethyl sulfoxide, and standard antibiotics such as ampicillin, streptomycin, and fluconazole, were used to validate the experimental setup. DMSO, used as a solvent control, exhibited high MIC values (>125 μg/μL) across most strains, indicating negligible intrinsic activity. Compared to the reference drugs, compounds **6d** and **6e** exhibited comparable or superior activity against several bacterial strains, highlighting their therapeutic potential.

Overall, the structure-activity relationship analysis suggests that the enhanced activity of **6d** and **6e** can be attributed to the introduction of electron-withdrawing groups and hydrophobic functionalities, which may facilitate stronger binding to microbial targets. These findings underscore the potential of these compounds as lead structures for developing new antimicrobial agents, warranting further investigations, including in vivo efficacy and toxicity studies.

Molecular docking studies. Molecular docking studies were conducted to evaluate the binding affinities and interactions of the synthesized triazole derivatives **6a**–**6e** with the bacterial DNA gyrase B enzyme (PDB ID: 4PRV). The molecular structures were optimized using Gaussian 09W at the DFT/B3LYP/6-31G(d,p) level,

ensuring their lowest energy conformations. The docking simulations, performed using AutoDock Vina, provided valuable insights into the potential binding modes and the interactions of the ligands within the active site of the target enzyme.

The docking results revealed significant variations in binding affinities among the compounds, with binding energies ranging from –7.9 (**6c**) to –9.9 kcal/mol (**6d**). Compound **6d** exhibited the strongest binding affinity (–9.9 kcal/mol), indicating its superior potential as a DNA gyrase B inhibitor. This can be attributed to its multiple interactions within the active site, three H-bond interactions were observed between the ligand and the active site with the amino acids CYS268, GLN275, and ARG276. π–σ Interaction was observed with the amino acids THR34 and ILE186, halogen interaction with the amino acid GLU193, and π–π interaction with the amino acid TYR267. The cumulative effect of these interactions likely stabilizes the ligand within the enzyme's active site, contributing to its potent inhibitory properties.

Compound 6e also showed strong binding affinity (–9.8 kcal/mol). After the docking study, two H-bond interactions were observed between the ligand and the active site with amino acids CYS268 and ARG276. It was observed that there was a π–π interaction with amino acid TYR267 and a π–σ interaction with amino acid ILE186. In addition, it was observed that there were π-alkyl interactions with amino acid ARG276. These interactions suggest that **6e** could serve as an alternative lead compound, with comparable inhibitory potential to **6d**. Compound **6b** demonstrated moderate binding affinity (–9.6 kcal/mol). It was observed that there were alkyl and π-alkyl interactions with amino acids LYS189, PRO274, and PHE41, carbon-hydrogen interactions with amino acids ARG276, ILE266, and GLN275, π-cation and π-anion interactions with amino acids GLU193 and ARG276, and π–π interactions with amino acid TYR267. The presence of fewer stabilizing interactions may account for its relatively lower affinity compared to **6d** and **6e**.

In contrast, compounds **6a** and **6c** displayed weaker binding affinities (–8.0 and –7.9 kcal/mol, respectively). Both compounds formed limited hydrogen bonds and relied primarily on weaker π-alkyl and π-donor interactions, suggesting less effective stabilization within the enzyme's active site. The results of the docking studies align with the structure-activity relationship observed in the antimicrobial evaluation. The enhanced activity of **6d** and **6e** can be attributed to their stronger binding affinities and extensive interactions with key residues within the DNA gyrase active site. The number and type of interactions, particularly hydrogen bonds and π–π stacking, appear to play a critical role in stabilizing the ligand-enzyme complex, thereby influencing the inhibitory potential of the compounds.

CONCLUSIONS

In this study, a series of novel 1,2,4-triazole derivatives **6a**–**6e** were successfully synthesized, characterized, and evaluated for their antimicrobial activity and molecular interactions with bacterial DNA gyrase B (PDB ID: 4PRV). The synthetic approach employed provided structurally diverse derivatives with high yields and purity, confirmed through FT-IR, NMR, and EI-MS analyses. The compounds demonstrated significant antimicrobial activity against both gram-positive and gram-negative bacteria, as well as fungal strains, with notable efficacy observed for compounds **6d** and **6e**.

The antimicrobial screening revealed that **6d** exhibited the highest potency, with MIC values as low as <0.24 μg/μL against all tested bacterial strains and strong activity against fungal pathogens such as *Saccharomyces cerevisiae* (15.65 μg/μL) and *Candida albicans* (62.5 μg/μL). The structure-activity relationship analysis highlighted that the presence of functional groups facilitating hydrogen bonding and hydrophobic interactions significantly enhanced the biological activity of the compounds.

Docking studies supported these findings, with **6d** emerging as the most promising inhibitor, showing the strongest binding affinity (–9.9 kcal/mol) to the DNA gyrase B enzyme. This was attributed to its multiple stabilizing interactions within the enzyme's active site, including three H-bond interactions were observed between the ligand and the active site with the amino acids CYS268, GLN275, and ARG276. π–σ Interaction was observed with the amino acids THR34 and ILE186, halogen interaction with the amino acid GLU193, and π–π interaction with the amino acid TYR267. Compound **6e** followed closely, exhibiting a binding energy of –9.8 kcal/mol, underscoring its potential as an alternative lead compound. The docking results aligned well with the antimicrobial data, reinforcing the reliability of the computational approach in predicting biological activity.

The combination of synthetic chemistry, antimicrobial evaluation, and molecular docking in this study underscores the potential of 1,2,4-triazole derivatives as promising candidates for antimicrobial drug development. Compound **6d** stands out as a lead structure with significant therapeutic potential. Future research will focus on further optimization of these compounds, in-depth pharmacokinetic studies, and in vivo assessments to validate their efficacy and safety. This integrated approach provides a strong foundation for the development of next-generation antimicrobial agents targeting bacterial DNA gyrase.

EXPERIMENTAL

All chemicals used in this study were purchased from Fluka Chemie AG (Buchs, Switzerland) and utilized without further purification. The melting points of the synthesized compounds were determined using a Büchi B-540 melting point apparatus with open capillaries, and the reported values were uncorrected. Reaction progress was monitored via thin-layer chromatography (TLC) performed on silica gel 60 F254 aluminum sheets. Visualization was achieved under UV light, and the mobile phase consisted of a 1 : 1 mixture of ethyl acetate and diethyl ether. Fourier-transform infrared (FT-IR) spectra were recorded on a PerkinElmer 1600 series spectrometer. Nuclear magnetic resonance (NMR) analyses were conducted in DMSO-d_6 using a Bruker Avance II 400 MHz spectrometer for ^{1}H NMR and 100 MHz for ^{13}C NMR spectra. Mass spectra were obtained through electron ionization (EI) using a Quattro GC-MS system operating at 70 eV. All synthesized compounds, including key intermediates, were subjected to antimicrobial screening to assess structure–activity relationships and track the evolution of biological activity throughout the synthetic pathway

Ethyl 2-(4-methylpiperazin-1-yl)acetate (2). A solution of methylpiperazine (1.14 g, 10.0 mmol, 1.0 equiv.) in tetrahydrofuran (10 mL) was prepared. To this, triethylamine (2.02 g, 20.0 mmol, 2.0 equiv.) and ethyl bromoacetate (1.51 g, 10.0 mmol, 1.0 equiv.) were added dropwise at room temperature. The reaction mixture was stirred for 24 h. After completion (monitored by TLC), the precipitated triethylammonium salt was removed by filtration. The filtrate was concentrated under reduced pressure, and the resulting crude residue was purified by column chromatography on silica gel using a hexane–ethyl acetate (7 : 3) eluent to afford ethyl 2-(4-methylpiperazin-1-yl)acetate as a colorless oil. Yield 1.73 g (89%), mp 85–87°C. IR spectrum, ν_{max}, cm^{-1}: 1734 (C=O). ^{1}H NMR spectrum (DMSO-d_6), δ, ppm: 1.17–1.20 m (3H, CH_3), 1.99 s (2H, CH_2), 2.14 s (2H, CH_2), 2.30 s (2H, CH_2), 3.17 s (2H, CH_2), 3.39 s (2H, CH_2), 4.06–4.10 m (3H, CH_3). ^{13}C NMR spectrum (DMSO-d_6), δ_C, ppm: 14.57 (CH_3), 46.17 (CH_3), 53.24 (CH_2), 55.06 (CH_2), 58.98 (CH_2), 60.20 (CH_2), 63.93 (CH_2), 170.36 (C=O). Mass spectrum (EI), *m/z* (I_{rel}, %): 187.14 (100) $[M + 1]^+$, 209.85 (70) $[M + Na]^+$.

2-(4-Methylpiperazin-1-yl)acetohydrazide (3). A solution of compound **2** (1.74 g, 10.0 mmol, 1.0 equiv.) in ethanol (15 mL) was refluxed with hydrazine hydrate (1.25 g, 25.0 mmol, 2.5 equiv.) for 15 h. Upon completion of the reaction (monitored by TLC), the solvent was evaporated under reduced pressure. The resulting crude product was purified by column chromatography on silica gel using hexane–ethyl acetate (7 : 3) eluent system to afford 2-(4-methylpiperazin-1-yl)acetohydrazide as a white solid. Yield 1.63 g (85%), mp 134–136°C. IR spectrum, ν_{max}, cm^{-1}: 1734 (C=O). ^{1}H NMR spectrum (DMSO-d_6), δ, ppm: 2.14 s (3H, CH_3), 2.30 s (2H, CH_2), 2.40 s (4H, $2CH_2$), 2.88 s (4H, $2CH_2$), 3.75 br. s (2H, NH_2), 8.84 s (1H, CH_2). ^{13}C NMR spectrum (DMSO-d_6), δ_C, ppm: 46.20 (CH_3), 53.21 ($2CH_2$), 55.01 ($2CH_2$), 60.37 (CH_2), 168.69 (C=O). Mass spectrum (EI), *m/z* (I_{rel}, %): 173.89 (100) $[M + 1]^+$, 195.75 (75) $[M + Na]^+$.

***N*-Benzyl-2-[(4-methylpiperazin-1-yl)acetyl]-hydrazinecarbothioamide (4).** A solution of compound **3** (1.59 g, 10.0 mmol, 1.0 equiv.) in dichloromethane (15 mL) was combined with benzyl isothiocyanate (1.49 g, 10.0 mmol, 1.0 equiv.). The reaction mixture was stirred continuously at room temperature for 24 h. During the reaction, a white precipitate began to form, indicating product formation. Upon completion (monitored by TLC), the solid product was collected by vacuum filtration, washed with cold dichloromethane (2 × 5 mL) to remove any impurities, and recrystallized from methanol (10 mL) to afford *N*-benzyl-2-[(4-methylpiperazin-1-yl)acetyl]-hydrazinecarbothioamide in high purity. Yield 2.62 g (81%), mp 139–141°C. IR spectrum, ν_{max}, cm^{-1}: 1703 (C=O), 3057 (CH_{Ar}), 3117 (NH), 3218 (NH). ^{1}H NMR spectrum (DMSO-d_6), δ, ppm: 1.86 s (3H, CH_3), 2.00 s (2H, CH_2), 2.17 s (2H, CH_2), 2.36 s (2H, CH_2), 2.47 s (2H, CH_2), 3.02 s (2H, CH_2), 4.72 s (2H, CH_2), 7.22–7.32 m (5H, H_{Ar}), 8.38 s (1H, NH), 8.50 s (1H, NH), 9.30 s (1H, NH). ^{13}C NMR spectrum (DMSO-d_6), δ_C, ppm: 45.97 (CH_3), 47.19 (CH_2), 47.40 (CH_2), 52.97 (CH_2), 54.81

(CH_2), 60.19 (CH_2), 63.96 (CH_2), 127.08 (CH), 127.48 (CH), 127.74 (CH), 128.44 (CH), 128.51 (CH), 139.70 (C), 169.58 (C=O), 182.63 (C=S). Mass spectrum (EI), *m/z* (I_{rel}, %)): 322.45 (100) $[M + 1]^+$, 201.26 (89), 178.10 (67), 166.10 (43).

4-Benzyl-5-[(4-methylpiperazin-1-yl)methyl]-4*H*-1,2,4-triazole-3-thiol (5). A solution of compound **4** (3.22 g, 10.0 mmol, 1.0 equiv.) in an ethanol–water mixture (1:1, 50 mL of ethanol and 50 mL distilled water) was refluxed in the presence of 20% aqueous NaOH (2.0 mL, 1.0 M NaOH, ~2.0 mmol, 0.2 equiv.) for 6 h. After completion of the reaction (monitored by TLC), the reaction mixture was cooled to room temperature, and the pH was carefully adjusted to 4 using concentrated HCl (37%, ~1.5 mL). The resulting precipitate was filtered under vacuum, washed thoroughly with cold distilled water (2 × 10 mL), and recrystallized from ethyl acetate (15 mL) to afford the pure compound 4-benzyl-5-[(4-methylpiperazin-1-yl)methyl]-4*H*-1,2,4-triazole-3-thiol. Yield 2.31 g (71%), mp 155–157°C. IR spectrum, ν_{max}, cm^{-1}: 2935 (SH), 3071 (CH_{Ar}). ^1H NMR spectrum (DMSO-d_6), δ, ppm: 2.17 s (3H, CH_3), 2.61 s (2H, CH_2), 4.29 d (2H, CH_2, *J* 8.0 Hz), 5.11 s (2H, CH_2), 5.19 s (2H, CH_2), 5.24 s (2H, CH_2), 5.32 s (2H, CH_2), 7.20–7.35 m (5H, H_{Ar}), 13.90 s (1H, SH). ^{13}C NMR spectrum (DMSO-d_6), δ_C, ppm: 11.72 (CH_3), 44.68 (CH_2), 45.83 (CH_2), 46.16 (CH_2), 46.65 (CH_2), 51.52 (CH_2), 52.69 (CH_2), 127.68 (CH), 127.92 (CH), 128.23 (CH), 128.58 (CH), 128.79 (CH), 152.53 (C), 164.84 (triazole C^3), 167.56 (triazole C^5).

General procedure for the synthesis of compounds 6a–6e. A solution of compound **5** (2.67 g, 10.0 mmol, 1.0 equiv.) in dimethyl sulfoxide (10 mL) was prepared. To this solution, the appropriate secondary amine (30.0 mmol, 3.0 equiv.; e. g., 2.61 g of morpholine) and formaldehyde solution (1.80 mL, 37% w/w, ~30.0 mmol, 3.0 equiv.) were added sequentially. The reaction mixture was stirred continuously at room temperature for 24 h. During the reaction, formation of a solid precipitate was observed, indicating progression. Upon completion (monitored by TLC), the precipitate was collected by vacuum filtration, washed with cold distilled water (2 × 10 mL), and air-dried. For further purification, the crude product was recrystallized from 10 mL mixture of dimethyl sulfoxide and water (1:1, v/v), yielding the final Mannich-base compound **6a–6e** in analytically pure form.

4-Benzyl-5-[(4-methylpiperazin-1-yl)methyl]-2-(morpholinomethyl)-2*H*-1,2,4-triazole-3(4*H*)-thione (6a). Yield 3.01 g (83%), mp 178–180°C. IR spectrum, ν_{max}, cm^{-1}: 1593 (C=N), 3088 (CH_{Ar}). ^1H NMR spectrum (DMSO-d_6), δ, ppm: 2.78 s (3H, CH_3), 3.37 s (10H, $5CH_2$), 3.59 s (10H, $5CH_2$), 5.04 s (2H, CH_2), 6.94 s (1H, H_{Ar}), 7.24–7.28 m (1H, H_{Ar}), 7.47 s (1H, H_{Ar}), 7.57 s (1H, H_{Ar}), 8.48 s (1H, H_{Ar}). ^{13}C NMR spectrum (DMSO-d_6), δ_C, ppm: 19.70 (CH_3), 20.25 (CH_2), 46.41 (CH_2), 47.03 (CH_2), 48.69 (CH_2), 49.78 (CH_2), 51.39 (CH_2), 53.78 (CH_2), 55.69 (CH_2), 57.23 (CH_2), 58.09 (CH_2), 59.11 (CH_2), 119.85 (CH), 120.21 (CH), 121.58 (CH), 122.03 (CH), 125.79 (CH), 130.52 (C), 161.20 (triazole C^3), 162.78 (triazole C^5). Mass spectrum (EI), *m/z* (I_{rel}, %): 403.89 (100) $[M + 1]^+$, 298.78 (85), 170.12 (51).

4-Benzyl-5-[(4-methylpiperazin-1-yl)methyl]-2-[(4-phenylpiperazin-1-yl)methyl]-2*H*-1,2,4-triazole-3(4*H*)-thione (6b). Yield 3.38 g (76%), mp 183–185°C. IR spectrum, ν_{max}, cm^{-1}: 1589 (C=N), 3073 (CH_{Ar}). ^1H NMR spectrum (DMSO-d_6), δ, ppm: 2.60 d (3H, CH_3, *J* 4.0 Hz), 2.95 d (2H, CH_2, *J* 4.0 Hz), 2.99 s (2H, CH_2), 3.14 s (2H, CH_2), 3.15 s (2H, CH_2), 3.42 s (12H, $6CH_2$), 5.13 s (2H, CH_2), 6.77 s (1H, H_{Ar}), 6.92 d (3H, H_{Ar}, *J* 8.0 Hz), 7.21–7.26 m (4H, H_{Ar}), 7.54–7.59 s (1H, H_{Ar}), 8.45 s (1H, H_{Ar}). ^{13}C NMR spectrum (DMSO-d_6), δ_C, ppm: 17.22 (CH_3), 46.07 (CH_2), 47.53 (CH_2), 48.67 (CH_2), 49.09 (CH_2), 50.51 (CH_2), 51.79 (CH_2), 52.65 (CH_2), 53.64 (CH_2), 56.79 (CH_2), 57.98 (CH_2), 60.49 (CH_2), 117.89 (CH), 118.69 (CH), 119.43 (CH), 120.31 (CH), 121.96 (CH), 122.49 (CH), 123.10 (CH), 125.80 (CH), 126.98 (CH), 129.03 (CH), 130.78 (C), 133.59 (C), 165.90 (triazole C^3), 167.59 (triazole C^5). Mass spectrum (EI), *m/z* (I_{rel}, %): 478.69 (100) $[M + 1]^+$, 219.46 (87), 173.41 (45).

4-Benzyl-2-[(furan-2-ylmethylamino)methyl]-5-[(4-methylpiperazin-1-yl)methyl]-2*H*-1,2,4-triazole-3(4*H*)-thione (6c). Yield 78%, mp 178–180°C. IR spectrum, ν_{max}, cm^{-1}: 1585 (C=N), 3093 (CH_{Ar}), 3210 (OH). ^1H NMR spectrum (DMSO-d_6), δ, ppm: 1.63 s (3H, CH_3), 2.74 s (2H, CH_2), 2.90 s (2H, CH_2), 3.13 s (2H, CH_2), 3.33 s (2H, CH_2), 3.41 s (4H, $2CH_2$), 3.62 s (2H, CH_2), 4.17 s (2H, CH_2), 7.26–7.33 m (5H, H_{Ar}), 7.96 s (1H, CH), 13.82 s (1H, NH). ^{13}C NMR spectrum (DMSO-d_6), δ_C, ppm: 16.10 (CH_3), 45.21 (CH_2), 46.52 (CH_2), 47.41 (CH_2), 48.96 (CH_2), 50.23 (CH_2), 51.73 (CH_2), 53.59 (CH_2), 54.90 (CH_2), 110.52 (CH), 112.36 (CH), 114.78 (CH), 115.37 (CH), 123.70 (CH), 139.07 (C), 142.43 (C), 163.89 (triazole C^3), 164.70 (triazole C^5). Mass spectrum (EI), *m/z* (I_{rel}, %): 413.87 (100) $[M + 1]^+$, 199.10 (66), 163.41 (49), 110.12 (31).

7-[4-({4-Benzyl-3-[(4-methylpiperazin-1-yl)-methyl]-5-thioxo-4,5-dihydro-1,2,4-triazol-1-yl}-methyl)piperazin-1-yl]-1-ethyl-6-fluoro-4-oxo-1,4-dihydroquinoline-3-carboxylic acid (6d). Yield 3.17 g (89%), mp 242–244°C. IR spectrum, ν_{max}, cm^{-1}: 1582 (C=N), 1725 (C=O), 1699 (C=O), 3095 (CH_{Ar}), 3410 (OH). ^1H NMR spectrum (DMSO-d_6), δ, ppm: 1.40 s (3H, CH_3), 2.73 s (3H, CH_3), 2.89 s (4H, $2CH_2$), 3.03 s (4H, $2CH_2$), 3.34 s (8H, $4CH_2$), 4.59 s (4H, $2CH_2$), 5.16 s (4H, $2CH_2$), 6.93 s (1H, H_{Ar}), 7.25 s (1H, H_{Ar}), 7.48 s (1H, H_{Ar}), 7.87–7.90 m (2H, H_{Ar}), 8.48 s (1H, H_{Ar}), 8.93 s (1H, CH), 15.35 s (1H, OH). ^{13}C NMR spectrum (DMSO-d_6), δ_C, ppm: 11.20 (CH_3), 17.52 (CH_3), 45.23 (CH_2), 45.98 (CH_2), 46.19 (CH_2), 46.89 (CH_2), 50.51 (CH_2), 51.97 (CH_2), 52.10 (CH_2), 52.88 (CH_2), 53.41 (CH_2), 54.41 (CH_2), 55.79 (CH_2), 56.70 (CH_2), 113.52 (CH), 114.79 (CH), 115.28 (CH), 117.34 (CH), 118.61 (CH), 119.39 (CH), 120.31 (CH), 128.41 (C), 129.80 (C), 130.76 (C), 131.31 (C), 132.70 (C), 133.74 (C), 161.67 (triazole C^3), 163.79 (triazole C^5), 170.46 (C=O), 173.52 (C=O). Mass spectrum (EI), *m/z* (I_{rel}, %): 635.78 (100) $[M+1]^+$, 510.42 (88), 413.89 (71), 217.52 (43).

7-[4-({4-Benzyl-3-[(4-methylpiperazin-1-yl)-methyl]-5-thioxo-4,5-dihydro-1,2,4-triazol-1-yl}-methyl)piperazin-1-yl]-1-cyclopropyl-6-fluoro-4-oxo-1,4-dihydroquinoline-3-carboxylic acid (6e). Yield 4.89 g (91%), mp 238–240°C. IR spectrum, ν_{max}, cm^{-1}: 1578 (C=N), 1718 (C=O), 1703 (C=O), 3089 (CH_{Ar}), 3421 (OH). ^1H NMR spectrum (DMSO-d_6), δ, ppm: 1.16 s (3H, CH_3), 1.30 s (2H, CH_2), 1.32 s (2H, CH_2), 3.05 s (2H, CH_2), 3.37 s (2H, CH_2), 3.80 s (14H, $7CH_2$), 5.16 s (2H, CH_2), 6.94 s (1H, H_{Ar}), 7.23–7.27 s (2H, H_{Ar}), 7.49–7.59 s (2H, H_{Ar}), 7.87–7.90 m (2H, H_{Ar}), 8.46 s (1H, CH), 8.65 s (1H, CH), 15.20 s (1H, OH). ^{13}C NMR spectrum (DMSO-d_6), δ_C, ppm: 13.41 (CH_3), 46.10 (CH_2), 47.13 (CH_2), 48.48 (CH_2), 49.11 (CH_2), 50.03 (CH_2), 50.77 (CH_2), 51.13 (CH_2), 52.78 (CH_2), 53.90 (CH_2), 54.78 (CH_2), 55.13 (CH_2), 56.41 (CH_2), 58.03 (CH_2), 112.70 (CH), 113.90 (CH), 115.03 (CH), 116.70 (CH), 119.63 (CH), 120.09 (CH), 121.10 (CH), 130.70 (C), 131.52 (C), 132.08 (C), 133.70 (C), 135.78 (C), 136.10 (C), 159.20 (triazole C^3), 160.41 (triazole C^5), 172.52 (C=O), 174.96 (C=O). Mass spectrum (EI), *m/z* (I_{rel}, %)): 647.89 (100) $[M+1]^+$, 488.10 (73), 310.41 (51), 170.43 (31).

2-{4-Benzyl-3-[(4-methylpiperazin-1-yl)methyl]-5-thioxo-4,5-dihydro-1,2,4-triazol-1-yl}-1-(4-chlorophenyl)ethanone (7). A mixture of compound **5** (2.67 g, 10.0 mmol, 1.0 equiv.) and sodium ethoxide (0.068 g, 1.0 mmol, 0.1 equiv.) was dissolved in ethanol (10 mL) and refluxed for 6 h. After this initial period, 2-bromo-1-(4-chlorophenyl)ethanone (2.05 g, 10.0 mmol, 1.0 equiv.) was added to the reaction mixture, and refluxing was continued for an additional 16 h to complete the reaction (monitored by TLC). The solvent was then evaporated under reduced pressure, and the crude product was isolated by filtration. The solid was washed with cold ethanol (2 × 5 mL) to remove any impurities and subsequently recrystallized from a 1 : 3 (v/v) mixture of acetone and water (20 mL total) to afford the target compound in high purity. Yield 4.56 g (90%), mp 203–205°C. IR spectrum, ν_{max}, cm^{-1}: 1598 (C=N), 1725 (C=O), 3097 (CH_{Ar}). ^1H NMR spectrum (DMSO-d_6), δ, ppm: 2.27 d (3H, CH_3, *J* 4.0 Hz), 2.40 s (2H, CH_2), 2.55 d (2H, CH_2, *J* 4.0 Hz), 3.39 s (2H, CH_2), 4.39 s (2H, CH_2), 4.57 s (2H, CH_2), 5.10 s (2H, CH_2), 5.48 s (2H, CH_2), 7.19 s (1H, H_{Ar}), 7.20 s (1H, H_{Ar}), 7.26 s (2H, H_{Ar}), 7.35 s (1H, H_{Ar}), 7.63 s (1H, H_{Ar}). ^{13}C NMR spectrum (DMSO-d_6), δ_C, ppm: 20.14 (CH_3), 45.98 (CH_2), 46.01 (CH_2), 47.13 (CH_2), 48.36 (CH_2), 49.48 (CH_2), 50.79 (CH_2), 51.29 (CH_2), 113.52 (CH), 114.42 (CH), 119.43 (CH), 120.12 (CH), 121.49 (CH), 123.20 (CH), 124.80 (CH), 127.94 (CH), 129.43 (CH), 134.12 (C), 136.41 (C), 137.49 (C), 151.14 (triazole C^3), 156.79 (triazole C^5), 171.10 (C=O). Mass spectrum (EI), *m/z* (I_{rel}, %): 456.12 (100) $[M+1]^+$, 288.12 (78), 197.12 (51).

4-Benzyl-2-[2-(4-chlorophenyl)-2-hydroxyethyl]-5-[(4-methylpiperazin-1-yl)methyl]-2*H*-1,2,4-triazole-3(4*H*)-thione (8). A solution of compound **7** (4.56 g, 10.0 mmol, 1.0 equiv.) in absolute ethanol (50 mL) was prepared. Sodium borohydride (1.13 g, 30.0 mmol, 3.0 equiv.) was added portion wise under stirring, and the reaction mixture was refluxed for 18 h to complete the reduction. After the reaction was complete (monitored by TLC), the mixture was cooled to room temperature, and the solvent was evaporated under reduced pressure to yield an oily residue. The crude product was recrystallized from a 1 : 3 (v/v) mixture of acetone and distilled water (20 mL total) to afford the reduced compound in pure form. Yield 3.24 g (71%), mp 128–130°C. IR spectrum, ν_{max}, cm^{-1}: 1585 (C=N), 3078 (CH_{Ar}), 3319 (OH). ^1H NMR spectrum (DMSO-d_6), δ, ppm: 2.30 s (3H, CH_3), 2.44 s (2H, CH_2), 2.48 s (4H, $2CH_2$), 2.68 s (2H, CH_2), 4.09 s (2H, CH_2), 4.63 s (2H, CH_2), 4.84 s (4H, $2CH_2$), 4.97 s (1H, CH), 5.26 s (1H, OH), 7.02 s (1H, H_{Ar}), 7.16 s (1H, H_{Ar}), 7.18 s (1H, H_{Ar}), 7.25 s (2H, H_{Ar}), 7.28 s (2H,

H_{Ar}), 7.36 s (2H, H_{Ar}). ^{13}C NMR spectrum (DMSO-d_6), δ_C, ppm: 20.90 (CH_3), 39.12 (CH_2), 46.56 (CH_2), 47.41 (CH_2), 49.03 (CH_2), 49.95 (CH_2), 50.07 (CH_2), 51.59 (CH_2), 126.12 (CH), 130.12 (CH), 131.19 (CH), 132.85 (CH), 133.76 (CH), 134.09 (CH), 135.90 (CH), 136.98 (CH), 137.12 (C), 138.90 (C), 140.52 (C), 153.70 (triazole C^3), 155.97 (triazole C^5). Mass spectrum (EI), *m/z* (I_{rel}, %): 458.90 (100) $[M + 1]^+$, 311.89 (73), 298.10 (55), 170.12 (41).

2-[2-(4-Chlorobenzyloxy)-2-(4-chlorophenyl)-ethyl]-4-benzyl-5-[(4-methylpiperazin-1-yl)methyl]-2*H*-1,2,4-triazole-3(4*H*)-thione (9). A solution of compound **8** (0.46 g, 1.0 mmol, 1.0 equiv) in tetrahydrofuran (10 mL) was prepared and cooled to 0°C. Sodium hydride (0.024 g, 1.0 mmol, 1.0 equiv, 60% dispersion in mineral oil) was added slowly under nitrogen atmosphere. The reaction mixture was then refluxed for 6 h to deprotonate the hydroxyl group. Subsequently, 4-chlorobenzylchloride (0.175 g, 1.0 mmol, 1.0 equiv.) was added dropwise, and the reaction was continued under reflux for an additional 10 h. Upon completion (monitored by TLC), the solvent was evaporated under reduced pressure, yielding a crude oily residue. This residue was stirred with an aqueous solution of potassium carbonate (0.138 g, 1.0 mmol, 10 mL) and extracted with ethyl acetate (3 × 15 mL). The combined organic layers were dried over anhydrous sodium sulfate, filtered, and concentrated under reduced pressure. The crude product was recrystallized from acetone (10 mL) to afford the final compound in pure form. Yield 0.34 g (58%), mp 69–71°C. IR spectrum, ν_{max}, cm^{-1}: 1579 (C=N), 3055 (CH_{Ar}), 3092 (CH_{Ar}). ^1H NMR spectrum (DMSO-d_6), δ, ppm: 2.27 s (3H, CH_3), 2.36 s (2H, CH_2), 2.39 s (4H, $2CH_2$), 2.57 s (2H, CH_2), 3.83 s (2H, CH_2), 4.45 s (2H, CH_2), 4.58 s (2H, CH_2), 4.65 s (2H, CH_2), 4.85 s (1H, CH), 5.08 s (1H, OH), 7.14–7.19 m (7H, H_{Ar}), 7.25–7.26 m (6H, H_{Ar}). ^{13}C NMR spectrum (DMSO-d_6), δ_C, ppm: 23.07 (CH_3), 40.63 (CH_2), 47.90 (CH_2), 48.66 (CH_2), 49.12 (CH_2), 50.88 (CH_2), 51.23 (CH_2), 52.44 (CH_2), 56.37 (CH_2), 119.10 (CH), 121.53 (CH), 123.20 (CH), 124.33 (CH), 126.50 (CH), 127.81 (CH), 128.64 (CH), 129.40 (CH), 134.39 (CH), 135.70 (CH), 136.86 (CH), 139.40 (CH), 141.33 (CH), 142.50 (CH), 143.23 (C), 144.03 (C), 145.30 (C), 146.23 (C), 147.34 (C), 148.78 (C), 156.89 (triazole C^3), 157.13 (triazole C^5). Mass spectrum (EI), *m/z* (I_{rel}, %): 582.29 (100) $[M + 1]^+$, 389.25 (73), 219.46 (57), 188.90 (40).

Antimicrobial activity assessment. The test microorganisms used in this study were obtained from the Hifzissihha Institute of Refik Saydam (Ankara, Turkey) and included *Escherichia coli* (ATCC35218), *Yersinia pseudotuberculosis* (ATCC911), *Pseudomonas aeruginosa* (ATCC43288), *Enterococcus faecalis* (ATCC29212), *Staphylococcus aureus* (ATCC25923), *Bacillus cereus* (709 Roma), *Mycobacterium smegmatis* (ATCC607), *Candida albicans* (ATCC60193), and *Saccharomyces cerevisiae* (RSKK 251). Stock solutions of the newly synthesized compounds were prepared by dissolving the compounds in DMSO at a concentration of 20 000 μg/mL.

The antimicrobial activities of the compounds were evaluated using the broth microdilution method to determine the minimum inhibitory concentration (MIC) values in μg/mL. Antibacterial testing was conducted in Mueller–Hinton broth (MH) (Difco, Detroit, MI) adjusted to pH 7.3, while antifungal testing was performed in buffered Yeast Nitrogen Base (Difco, Detroit, MI) at pH 7.0. For *Mycobacterium smegmatis*, Brain Heart Infusion broth (BHI) (Difco, Detroit, MI) was used as the growth medium, and plates were incubated for 48–72 h at 35°C. Other test microorganisms were incubated for 18–24 h at 35°C [27].

Ampicillin (10 μg/mL) and fluconazole (5 μg/mL) were used as standard antibacterial and antifungal drugs, respectively, to compare the antimicrobial effects of the synthesized compounds. Dimethyl sulfoxide diluted to 1 : 10 served as the solvent control. All tests were performed in triplicate to ensure reproducibility, and the results are presented in Table 1.

The antimicrobial testing of intermediates provided useful comparative insights, demonstrating that successive structural modifications significantly influenced bioactivity, with the final triazole derivatives exhibiting superior potency.

Stock solutions of the synthesized compounds were prepared at 20 000 μg/mL in DMSO to enable broad-range two-fold serial dilutions for MIC determination. Despite the higher initial stock concentration, all compounds were tested across equivalent dilution ranges, ensuring accurate comparison with standard drugs prepared at lower stock concentrations

Docking calculations. The molecular structures of the synthesized compounds **6a**–**6e** were optimized using Gaussian 09W, a quantum mechanical software designed for modeling a wide range of molecular systems.

Geometry optimizations were performed in the gas phase using density functional theory (DFT) with the B3LYP/6-31G(d,p) basis set. The optimized structures were converted into .pdb format for docking studies using GaussView 5.0 as the graphical interface. This process ensured that the molecules were in their minimum energy conformations, suitable for accurate docking simulations [28, 29].

Subsequently, the .pdb files were opened in AutoDock Tools (ADT) for further preparation. The torsion roots and the number of rotatable bonds in the ligands were determined, and the structures were saved in .pdbqt format, which is compatible with AutoDock Vina for docking simulations.

The target enzyme for docking studies was chosen based on structural and functional criteria obtained from the RCSB Protein Data Bank. Among several available structures, the 4PRV structure of *Escherichia coli* DNA gyrase B was selected. This structure, resolved at a resolution of 2.00 Å using X-ray crystallography, represents the 43-kDa *N*-terminal fragment of the DNA gyrase complexed with ADP and Mg ions. DNA gyrase B is a validated target for antibacterial drugs, given its essential role in bacterial DNA replication and transcription. The choice of 4PRV was further supported by its absence of mutations and detailed structural annotations, making it ideal for docking studies.

The docking methodology was validated using the 4PRV structure and its co-crystallized ligand, ADP. The ligand was extracted from the active site, and a redocking procedure was performed using AutoDock Vina. The root means square deviation (RMSD) between the docked and the original ADP ligand was calculated to be 1.425 Å, which is within the acceptable range (<2 Å), confirming the accuracy and reliability of the docking protocol for the selected system.

Docking simulations were performed using AutoDock Vina to evaluate the binding affinities and interactions of the synthesized compounds **6a**–**6e** with the 4PRV target enzyme. The configuration file contained details of the ligand and enzyme files, grid coordinates, and box dimensions. Each docking simulation generated nine potential conformations for each compound, and the binding energies were calculated. Results were analyzed using ADT, and key interactions were identified. The docking results of the synthesized compounds are given in detail in Table S1 (see Supplementary Information).

AUTHOR INFORMATION

Y.U. Cebeci, ORCID: https://orcid.org/0000-0001-7949-0329

FUNDING

This work was supported by ongoing institutional funding. No additional grants to carry out or direct this particular research were obtained.

CONFLICT OF INTEREST

The authors of this work declare that they have no conflicts of interest.

SUPPLEMENTARY INFORMATION

The online version contains supplementary material available at https://doi.org/10.1134/S1070363225602820.

REFERENCES

1. Brown, E.D. and Wright, G.D., *Nature*, 2016, vol. 529, p. 336. https://doi.org/10.1038/nature17042
2. Lewis, K., *Nat. Rev. Drug Discov.*, 2013, vol. 12, p. 371. https://doi.org/10.1038/nrd3975
3. Gupta, R., Tandon, N., Gaba, A., Singh, R., and Mahajan, M., *Eur. J. Med. Chem.*, 2020, vol. 188, p. 112030. https://doi.org/10.1016/j.ejmech.2020.112030
4. El-Faham, A., Almarhoon, Z.M., Soliman, S.M., Ghabbour, H.A., Fun, H.K., and Al-Omar, M.A., *J. Adv. Res.*, 2021, vol. 32, p. 255. https://doi.org/10.1016/j.jare.2021.02.001
5. Ayyadurai, K., Perumal, S., Ramesh, P., Mahapatra, M.K., and Subramanian, V., *Bioorg. Med. Chem. Lett.*, 2021, vol. 31, p. 127710. https://doi.org/10.1016/j.bmcl.2020.127710
6. Sadiq, A., Mahnashi, M.H., Alyami, H.S., Alqahtani, Y.S., Jan, M.S., Ullah, R., and Khan, A., *J. Med. Chem.*, 2022, vol. 65, p. 5634. https://doi.org/10.1021/acs.jmedchem.2c00103
7. Hooper, D.C., *Drug Resist. Updat.*, 1999, vol. 2, p. 38. https://doi.org/10.1054/drup.1998.0068
8. Drlica, K. and Zhao, X., *Microbiol. Mol. Biol. Rev.*, 1997, vol. 61, p. 377. https://doi.org/10.1128/MMBR.61.3.377-392.1997

9. Khursheed, R., Rather, M.A., Dar, A.H., Malik, A., Madni, A., and Ali, A., *Chem. Biol. Drug Des.*, 2022, vol. 99, p. 134. https://doi.org/10.1111/cbdd.14037
10. Ghorab, M., Alsaid, M.S., El-Gazzar, M.G., Safwat, N.A., and El-Sayed, N., *Eur. J. Med. Chem.*, 2019, vol. 185, p. 111825. https://doi.org/10.1016/j.ejmech.2019.111825
11. Chopra, I., Schofield, C., Everett, M., O'Neill, A., Miller, K., Wilcox, M., Frère, J.M., Dawson, M., Czaplewski, L., Urleb, U., Courvalin, P., Berger-Bächi, B., Piddock, L.J.V., Fisher, L., MacGowan, A., Hunter, P., Williams, D.H., White, T., Darby, G., and Bax, R., *Lancet Infect. Dis.*, 2001, vol. 1, p. 194. https://doi.org/10.1016/S1473-3099(01)00122-0
12. Sutherland, R., Croydon, E.A., and Rolinson, G.N., *J. Antimicrob. Chemother.*, 1982, vol. 9, p. 114. https://doi.org/10.1093/jac/9.2.114
13. Schimel, D., *Nat. Med.*, 2014, vol. 20, p. 832. https://doi.org/10.1038/nm0814-832
14. Golan, Y., Wolf, M.P., Pauker, S.G., and Wong, J.B., *J. Intensive Care Med.*, 2012, vol. 27, p. 74. https://doi.org/10.1177/0885066610393632
15. Singh, R., Garg, N., Tiwari, A., Yadav, P., and Srivastava, P., *J. Enzyme Inhib. Med. Chem.*, 2020, vol. 35, p. 1578. https://doi.org/10.1080/14756366.2020.1800301
16. Zhu, Y., He, Z., Tang, Y., Xu, Y., and Xu, H., *J. Chem. Inf. Model.*, 2021, vol. 61, p. 2110. https://doi.org/10.1021/acs.jcim.1c00262
17. Black, T.A. and Blondeau, J.M., *Clin. Microbiol. Rev.*, 2001, vol. 14, p. 199. https://doi.org/10.1128/CMR.14.2.199-221.2001
18. Lewis, K., Lester, R., O'Neill, A.J., Miller, K., MacLean, R.C., and Brown, E.D., *Annu. Rev. Med.*, 2015, vol. 66, p. 397. https://doi.org/10.1146/annurev-med-070613-123343
19. Baquero, F. and Coque, T.M., *Microb. Biotechnol.*, 2011, vol. 4, p. 523. https://doi.org/10.1111/j.1751-7915.2011.00268.x
20. Fischbach, M.A. and Walsh, C.T., *Science*, 2009, vol. 325, p. 1089. https://doi.org/10.1126/science.1176667
21. Lipinski, C.A., Lombardo, F., Dominy, B.W., and Feeney, P.J., *Adv. Drug Deliv. Rev.*, 2001, vol. 46, p. 3. https://doi.org/10.1016/S0169-409X(00)00129-0
22. RCSB Protein Data Bank, RCSB Database. (Accessed September 24, 2025) https://www.rcsb.org
23. Pommier, Y., Leo, E., Zhang, H., and Marchand, C., *Nat. Rev. Cancer*, 2010, vol. 10, p. 741. https://doi.org/10.1038/nrc2910
24. Park, S.Y., Kim, H., Kim, J., and Lee, K., *Comput. Biol. Chem.*, 2022, vol. 99, p. 107712. https://doi.org/10.1016/j.compbiolchem.2022.107712
25. Frisch, M.J., Trucks, G.W., Schlegel, H.B., Scuseria, G.E., Robb, M.A., Cheeseman, J.R., Scalmani, G., Barone, V., Mennucci, B., Petersson, G.A., Nakatsuji, H., Caricato, M., Li, X., Hratchian, H.P., Izmaylov, A.F., Bloino, J., Zheng, G., Sonnenberg, J.L., Hada, M., and Fox, D.J., *Gaussian09W*, Gaussian Inc., 2016.
26. Trott, O., and Olson, A.J., *J. Comput. Chem.*, 2010, vol. 31, p. 455. https://doi.org/10.1002/jcc.21334
27. Willanova, M., *National Committee for Clinical Laboratory Standards. Methods for Determining Bactericidal Activity of Antibacterial Agents,* App. Guid. NCCLS, 1999, vol. 18.
28. Frisch, M.J., Trucks, G.W., Schlegel, H.B., Scuseria, G.E., Robb, M.A., Cheeseman, J.R., Scalmani, G., Barone, V., Mennucci, B., Petersson, G.A., Nakatsuji, H., Caricato, M., Li, X., Hratchian, H.P., Izmaylov, A.F., Bloino, J., Zheng, G., Sonnenberg, J.L., Hada, M., and Fox, D.J., *Gaussian 09, Revision A.02*, Gaussian Inc., 2016.
29. Nielsen, A.B. and Holder, A.J., Gaussian Inc., 2009, GaussView 5.0 User's Reference.

AI tools may have been used in the translation or editing of this article.